Light propagation in structural anisotropic media in the steady-state and time domains

Alwin Kienle, Florian Foschum, Ansgar Hohmann

Institut für Lasertechnologien in der Medizin und Meßtechnik, Helmholtzstraße 12, 89081 Ulm, Germany

E-mail: alwin.kienle@ilm.uni-ulm.de

Abstract. The determination of the reduced scattering and absorption coefficients of structural anisotropic turbid semi-infinite media and slabs was investigated in the steady-state and time domains. Forward calculations were performed with a Monte Carlo model that considered both cylindrical scatterers aligned in different directions as well as scatterers that were described by a rotationally symmetric scattering function. Analytical solutions of the isotropic and anisotropic diffusion equations were applied to retrieve the optical properties. It was found in the steady-state and time domains that the solutions of the anisotropic diffusion equation have systematic errors compared to the Monte Carlo simulations not only for small distances from the source. However, it is shown that in the time domain it is possible to retrieve useful values for the optical properties using the isotropic and the anisotropic diffusion equations.

PACS numbers: 07.05.TP, 87.64.K-, 78.20.Ci, 87.10.Rt, 87.64.Aa

Keywords: anisotropic light propagation, Monte Carlo simulation, optical properties, biological media

Submitted to: *Phys. Med. Biol.*

1. Introduction

The light propagation in scattering media is usually described with isotropic models for which it is assumed that the light scattering coefficient and the scattering function are independent of the light's incident direction [1, 2, 3]. However, many scattering media have an aligned microstructure which causes an anisotropic light propagation. Examples are liquid crystals [4, 5, 6, 7], textil material [8], or biological tissue such as skin [9, 10], dentin [11], muscles [12] or wood [13].

In literature mostly the anisotropic diffusion theory was used to describe the light propagation in these scattering media [4, 6, 7, 14, 15, 16, 17, 18, 19]. In addition, Monte Carlo simulations were applied to solve the more exact radiative transport equation. First studies were made with an approximated model to investigate the light

propagation in skin [9]. Subsequently, we introduced Monte Carlo simulations which considered, besides rotationally symmetric scattering functions, those of cylinders which were derived by analytical solutions of Maxwell's equations [11, 20]. As many parts of the body have cylindrical scatterers like collagen fibers, dentinal tubules or muscle fibers, this model can be applied for many tissue types. Later, the model was extended to the calculation of anisotropic light propagation of polarized light [21, 22, 23]. Instead of cylindrical scatterers also oriented ellipsoids were applied to calculate the anisotropic light propagation with the Monte Carlo method [24]. Further, a random walk model for anisotropic light propagation was introduced [25] and the anisotropic light propagation was studied for rendering purposes [26]. In addition, the Monte Carlo simulations were used to study the transport of seismic waves [27].

Besides forward calculations of the light propagation knowing the optical properties of the considered scattering medium, the important inverse problem, the determination of the optical properties of scattering media from reflectance or transmittance data, has been considered. For example, Johnson et al. applied the solution of the anisotropic diffusion equation for time resolved transmittance measurements from a slab to derive the reduced scattering and absorption coefficients [14]. Later the same group used the solution of the anisotropic diffusion equation in the steady-state domain to derive the scattering properties of a porous plastic fiber sample [28]. Recently, Alerstam and Svensson investigated powder compacts in the time domain using the anisotropic diffusion theory [29, 30] for determination of the reduced scattering coefficients. In literature mostly consistent results within the diffusion theory were reported, but, in general, the results were not checked against the actual optical properties. We considered this issue by fitting the solution of the isotropic diffusion equation to reflectance from semi-infinite anisotropic media calculated by the Monte Carlo method. Using this approach we showed that in the time domain it is possible to derive the absorption coefficient with good accuracy [31], whereas for steady state measurements we found that the optical coefficients cannot be derived correctly [31, 32].

In the present study we extended our earlier work [31] in several directions. Firstly, the anisotropic light propagation was investigated not only for semi-infinite but also for laterally infinitely extended slab geometries using Monte Carlo simulations that consider aligned cylindrical and random scatterers. Secondly, besides analytical solutions of the isotropic diffusion equation also those of the anisotropic diffusion equation were applied to derive the reduced scattering and the absorption coefficients in the steady-state and the time domains. Thirdly, the prediction of the diffusion theory that the time resolved transmittance from a slab at the opposite side of the perpendicularly incident delta pulse does not depend on the reduced scattering coefficient parallel to the slab is investigated with the Monte Carlo method.

2. Methods

2.1. Monte Carlo simulations

In this study it is assumed that the radiative transport equation can be used to correctly study the light propagation in scattering media [33]. The Monte Carlo method is applied to solve this equation numerically. Simulations were performed for the spatially resolved and time resolved reflectance from semi-infinite media and for the spatially resolved and time resolved reflectance and transmittance from laterally infinitely extended slabs. The thickness of the considered slabs were varied, however, because of conciseness only the results of the slab with a thickness of 10 mm are presented. In order to cause an anisotropic light propagation cylindrical scatterers were simulated. Three different models for the microscopic arrangement of the scatterers were investigated. First, all cylinders were aligned in z-direction, which corresponds to the direction of the δ-source incident perpendicularly to the boundary of the considered media, see Fig. 1. Besides cylinders, this model also consisted of non-aligned scatterers, which were described by the Henyey-Greenstein function using an anisotropy factor of $g = 0.8$ and a reduced scattering coefficient of $\mu_s' = 1\,\mathrm{mm}^{-1}$. The second and third models consisted of cylinders which were aligned with a probability of 50% in x-direction and 50% in y-direction, and 75% in x-direction and 25% in y-direction, respectively. For the latter two models no scatterers which are described by rotationally symmetric scattering function were considered. The scattering functions for the cylinders were obtained by an analytical solution of Maxwell's equations [34]. Two types of cylinders were studied. The first type corresponding to tubules in dentin had a diameter of $2\,\mu$m and a refractive index of 1.33, whereas the refractive index used for the material outside the cylinder was 1.52 and the wavelength was $\lambda = 633\,$nm. For the refractive index of the whole medium 1.5 was assumed. The second type represented cylindric collagen fibers in tendon. The cylinders had a diameter of $3\,\mu$m and a refractive index of 1.46. Outside the cylinder and for the whole scattering medium a refractive index of 1.36 was applied. The assumed wavelength was $\lambda = 800\,$nm. For the refractive index outside the scattering media a refractive index of 1.0 was used for all cases. Due to the better statistics almost all graphs presented in the 'Results' section were obtained from the model of the dentinal tubules. Different concentrations of the cylindrical tubules were applied. In this study the used concentrations of tubules were expressed in terms of $c_0 = 9260\,\mathrm{mm}^{-2}$. In all presented simulations the absorption coefficient was set to $\mu_a = 0.01\,\mathrm{mm}^{-1}$.

For the simulation of the scattering interaction the scattering coefficient for the actual photon direction was calculated by adding μ_s due to the non-aligned scatterers and μ_s due to the cylinders. The latter was obtained by multiplying the scattering cross section of the cylinders for the angle between the actual photon direction and the cylinders axes, ξ, times the cylinder's concentrations. This was done for each group of cylinders aligned in different directions, if present. The scattering cross sections were calculated by the analytical solution of Maxwell's equations [34]. The actual scattering length was computed from the summed scattering coefficient. Then, using the random

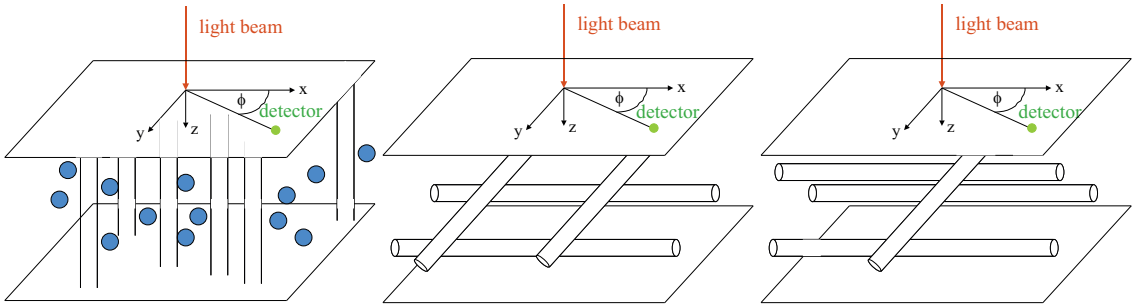

Figure 1. Schemes of model 1 (left), model 2 (central), and model 3 (right) of the structural anisotropic media investigated in this study.

number generator it was decided if the photon was scattered by a cylinder having a certain direction or by the non-aligned scatterers, if present. The new scattering direction was calculated by the scattering function obtained again by the analytical solution of Maxwell's equations for the actual angle ξ. The new position of the next scattering interaction was found by using an adequate coordinate transformation. In order to verify the results two (by two of the authors) completely independently written Monte Carlo codes were compared.

2.2. Diffusion theory

The steady-state domain and time domain solutions of the isotropic and anisotropic diffusion equations were used to retrieve the optical properties. In the time domain the reflectance $R(x, y, t)$ and transmittance $T(x, y, t)$ from a laterally infinitely extended slab with a thickness of l_z were calculated using

$$\begin{aligned} U(x,y,t) \quad &= \frac{1}{2}(D_x D_y D_z)^{-0.5}(4\pi c)^{-3/2} t^{-5/2} \exp\left(-\frac{x^2}{4D_x ct} - \frac{y^2}{4D_y ct} - \mu_a ct\right) \\ &\times \sum_{n=-\infty}^{\infty} \left((u - z_{1n}) \exp\left(-\frac{(u-z_{1n})^2}{4D_z ct}\right) - (u - z_{2n}) \exp\left(-\frac{(u-z_{2n})^2}{4D_z ct}\right)\right), \end{aligned} \tag{1}$$

with $R(x, y, t) = -U(x, y, t)$ setting $u = 0$ and with $T(x, y, t) = U(x, y, t)$ setting $u = l_z$, respectively. $D_x = 1/(3\mu'_{sx})$, $D_y = 1/(3\mu'_{sy})$, and $D_z = 1/(3\mu'_{sz})$ are the xx-, yy-, and zz-components of the diffusion tensor and $c = c_v/n$ is the velocity of light in the considered medium having the refractive index n, which was assumed to be independent of the direction, and c_v being the velocity of light in vacuum. Further, z_{1n} and z_{2n} are given by

$$\begin{aligned} z_{1n} &= 2nl_z + 4nz_b + z_0 \ , \\ z_{2n} &= 2nl_z + (4n-2)z_b - z_0 \ , \end{aligned} \tag{2}$$

where $z_0 = 1/(\mu'_{sz} + \mu_a)$, $z_b = \frac{1+R_{eff}}{1-R_{eff}} \frac{2}{3\mu'_{sz}}$ and R_{eff} represents the fraction of the photons that is internally diffusely reflected at the boundary [35].

The steady-state spatially resolved reflectance and transmittance were calculated using

$$
\begin{aligned}
U(x,y) = \frac{1}{4\pi\sqrt{D_x D_y D_z}} \sum_{n=-\infty}^{\infty} & \\
& \left((u - z_{1n}) \left(\left(\frac{x^2}{D_x} + \frac{y^2}{D_y} + \frac{(u-z_{1n})^2}{D_z} \right)^{-0.5} + \sqrt{\mu_a} \right) \right. \\
& \times \frac{\exp(-\sqrt{\mu_a}\sqrt{\frac{x^2}{D_x} + \frac{y^2}{D_y} + \frac{(z-z_{1n})^2}{D_z}}}{\frac{x^2}{D_x} + \frac{y^2}{D_y} + \frac{(u-z_{1n})^2}{D_z}} \\
& -(u - z_{2n}) \left(\left(\frac{x^2}{D_x} + \frac{y^2}{D_y} + \frac{(u-z_{2n})^2}{D_z} \right)^{-0.5} + \sqrt{\mu_a} \right) \\
& \left. \times \frac{\exp(-\sqrt{\mu_a}\sqrt{\frac{x^2}{D_x} + \frac{y^2}{D_y} + \frac{(z-z_{2n})^2}{D_z}}}{\frac{x^2}{D_x} + \frac{y^2}{D_y} + \frac{(u-z_{2n})^2}{D_z}} \right) ,
\end{aligned}
\tag{3}
$$

with $R(x,y) = -U(x,y)$ setting $u = 0$ and with $T(x,y) = U(x,y)$ setting $u = l_z$, respectively. For the derivation of the reflectance and transmittance of both domains Fick's law was used [35]. From the above equations the solutions for the isotropic diffusion equations was obtained by setting $D_x = D_y = D_z$. For describing rotationally symmetric contour lines of the reflectance and transmittance $D_r = D_x = D_y$ was used. Finally, the solutions of the reflectance from a semi-infinite geometry were obtained by applying $l_z \to \infty$, from which follows that only two terms of the sum over n are retained.

3. Results

3.1. Steady-state Domain

The iso-intensity contour lines of the spatially resolved reflectance and transmittance obtained from the Monte Carlo simulations for model 1 are circles due to the direction of the cylinders in z-direction. For models 2 and 3 the iso-intensity contour lines are more involved. Fig. 2 shows the contour lines for the reflectance from a slab having a thickness of 10 mm for model 2 (left figure) and model 3 (right figure). The cylindrical scatterers having a concentration of c_0 represent dentinal tubules as in the whole subsection. At small distances from the incident pencil beam the contour lines are influenced strongly by the single scattering behavior of the cylinders. Cylinders which are aligned in x- and in y-directions cause iso-intensity contour lines elongated in y- and in x-directions, respectively [20]. For an equal number of cylinders in both directions this leads to square-like contour lines for small distances from the source (left figure), whereas the higher number of cylinders in x-direction causes ellipse-like contour lines elongated in y-direction for small distances (right figure). For large distances the contour lines

approximate a circle for model 2 and an ellipse elongated in x-direction for model 3. We note that the latter geometrical patterns are attained at distances where the reflectance is already about 3 orders of magnitude smaller than the reflectance close to the incident source. Thus, having in mind that the solutions of the anisotropic diffusion equation deliver iso-intensity contour lines that are circles for model 2 ($\mu'_{sx} = \mu'_{sy}$; $\mu'_{sz} = \mu'_{sx} + \mu'_{sy}$) and ellipses for model 3 ($\mu'_{sx} = \mu'_{sy}/3$; $\mu'_{sz} = \mu'_{sx} + \mu'_{sy}$), compare Eq. 1, for all distances from the source it is obvious that diffusion theory cannot describe even qualitatively these contour lines for the overwhelming part of the remitted light. Quantitatively, the diffusion theory predicts elliptical patterns for model 3 with a ratio of $\sqrt{3} = 1.73$ for the semi-axes because there are 3 times more cylinders in x- than in y-directions, compare Eq. 3. With the Monte Carlo simulation smaller ratios are obtained even for large distances. For example, the iso-intensity contour line for $0.0001\,\mathrm{mm}^{-2}$ has a ratio of 1.61 ± 0.01.

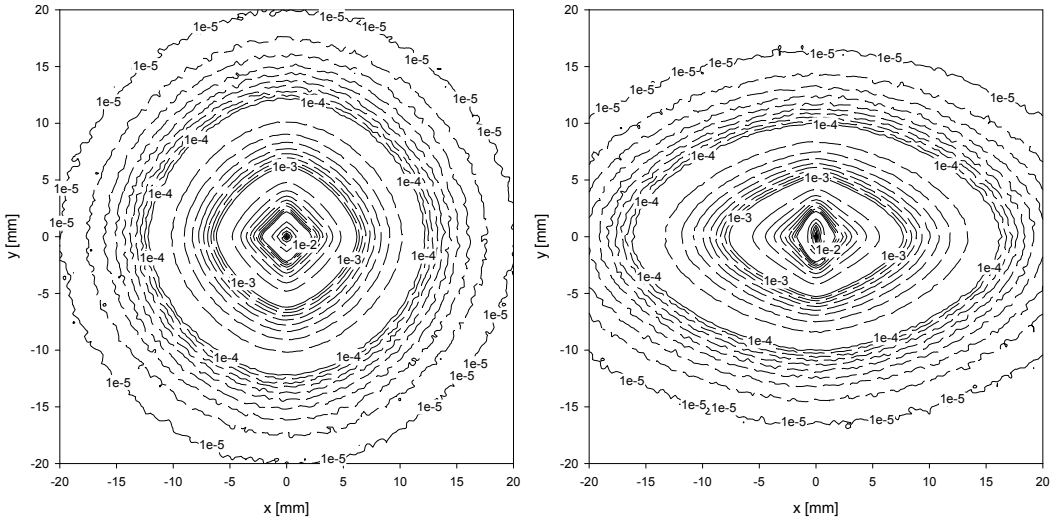

Figure 2. Two-dimensional spatially resolved reflectance (given in mm^{-2}) from turbid slabs consisting of aligned tubules which are illuminated perpendicularly by a $\delta(x, y)$-source. Further optical coefficients were $\mu_a = 0.01\,\mathrm{mm}^{-1}$ and $n = 1.5$. The thickness of the slab was 10 mm. In the left figure corresponding to model 2 the tubules were aligned 50% in x- and 50% in y-directions (both having a concentration of $c_0/2$) and in the right figure corresponding to model 3 75% in x- and 25% in y-direction (having a concentration of $3c_0/4$ and $c_0/4$, respectively).

For the remaining part of this subsection we present results obtained for model 1. As stated above, due to symmetry reasons ($\mu'_{sx} = \mu'_{sy}$) model 1 delivers circular iso-contour lines. The circular patterns are also obtained by the anisotropic diffusion equation in this case. In addition, due to the rotationally symmetric contour lines the spatially resolved reflectance or transmittance can be fully characterized by plotting the reflectance versus the distance to the source. Fig. 3 shows the spatially resolved reflectance from a turbid slab for four different concentrations ($c_0/\infty, c_0/2, c_0, 2c_0$) of the tubules calculated with the Monte Carlo method (solid curves) and with the anisotropic diffusion equation

(dashed lines). For a dentinal tubule concentration of c_0 aligned in z-direction the reduced scattering coefficients become approximately $\mu'_{sx} = \mu'_{sy} = 1.7\,\mathrm{mm}^{-1}$ and $\mu'_{sz} = 0\,\mathrm{mm}^{-1}$ for the anisotropic diffusion theory according to [36], which results in the following reduced scattering coefficients $\mu'_{sr} = \mu'_{sx} = \mu'_{sy} = 2.7\,\mathrm{mm}^{-1}$ and $\mu'_{sz} = 1\,\mathrm{mm}^{-1}$ for the whole medium considering also the Henyey-Greenstein scatterers which contribute equally to the different reduced scattering coefficients. Using these values for the anisotropic diffusion theory we found large differences compared to the Monte Carlo method for all distances (data only shown for $2c_0$ ($\mu'_{sr} = 4.4\,\mathrm{mm}^{-1}$)). By changing the reduced scattering coefficients for the cylindrical tubules we found that a good agreement was obtained with $\mu'_{sx} = \mu'_{sy} = 1.5\,\mathrm{mm}^{-1}$ for large distances, see Fig. 3.

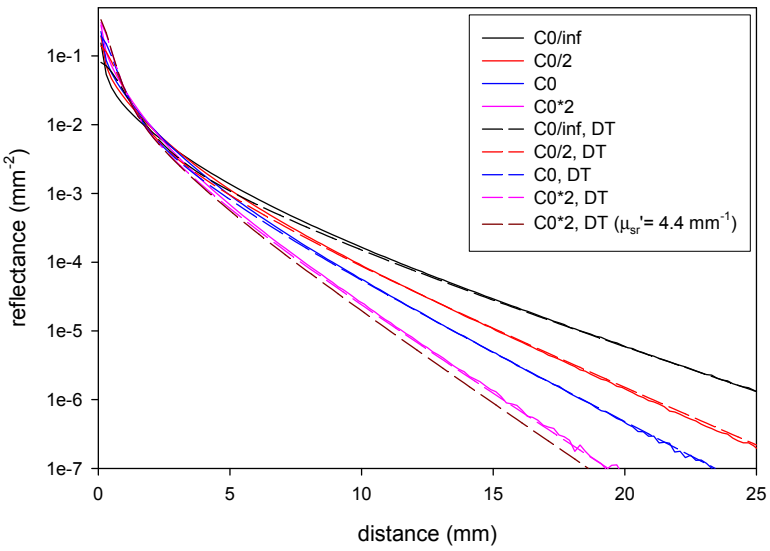

Figure 3. Spatially resolved reflectance from a turbid slab consisting of aligned tubules in z-direction which is illuminated by a $\delta(\rho)$-source. Calculations were performed with the Monte Carlo method for four different cylinder concentrations $(c_0/\infty, c_0/2, c_0, 2c_0)$. In addition, non-aligned scatterers were assumed which are described by $\mu'_s = 1\,\mathrm{mm}^{-1}$ and a Henyey-Greenstein scattering function with $g = 0.8$. The other optical coefficients were $\mu_a = 0.01\,\mathrm{mm}^{-1}$ and $n = 1.5$. The thickness of the slab was 10 mm. Further, the corresponding results from the anisotropic diffusion equations are shown ($\mu'_{sz} = 1.0\,\mathrm{mm}^{-1}$, $\mu'_{sr} = 1.0/1.75/2.5/4.0\,\mathrm{mm}^{-1}$). In addition, the spatially resolved reflectance for a concentration of $2c_0$ using $\mu'_{sz} = 1.0\,\mathrm{mm}^{-1}$ and $\mu'_{sr} = 4.4\,\mathrm{mm}^{-1}$ is given.

The figure shows that when the scattering medium does not contain any cylindrical scatterers (c_0/∞), i.e. when the light propagation is not anisotropic, the solution of the diffusion equation approximates the results from the Monte Carlo method for large distances as is well known [37]. A similar behavior is obtained for the comparison with the different non-zero cylinder concentrations. We note that for smaller distances ($< 15\,\mathrm{mm}$) a better agreement is obtained by not only using the flux term due to Fick's law but also the fluence term [37].

The spatially resolved transmittance for the same turbid slabs that were presented

in Fig. 3 are shown in Fig. 4 using the same reduced scattering coefficients. A good agreement between the anisotropic diffusion equation and Monte Carlo simulations is obtained. The larger the concentration of the tubules the larger is the intensity of the spatially resolved transmittance at small distances and the faster is the lateral decrease. Thus, the increase of the cylinder concentration leads to a light guiding effect caused by scattering, compare [38], which is even more obvious when the data are depicted in a linear scale, see inset of Fig. 4. In addition, the spatially resolved transmittance obtained with the independently written second Monte Carlo code is depicted for a concentration of c_0 showing an agreement within the noise of the simulations.

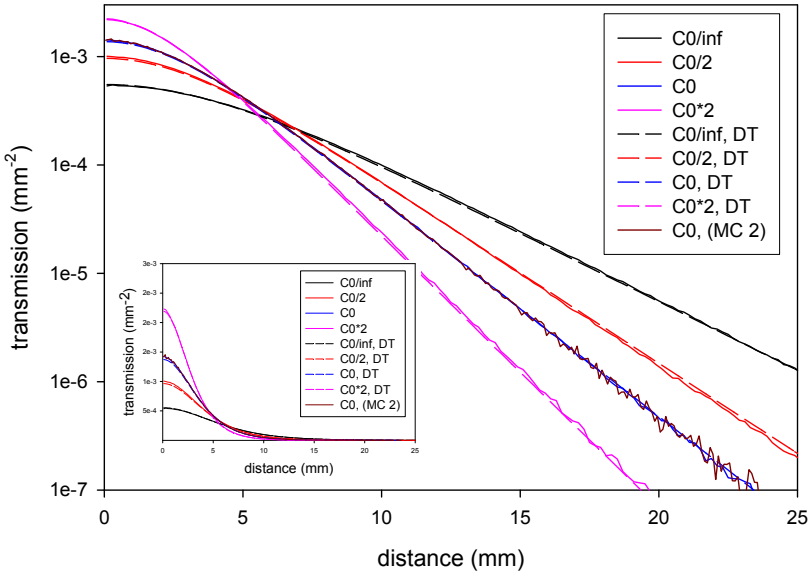

Figure 4. Spatially resolved transmittance from a turbid slab consisting of aligned tubules in z-direction which is illuminated by a $\delta(\rho)$-source. Calculations were performed with the Monte Carlo method for four different cylinder concentrations $(c_0/\infty, c_0/2, c_0, 2c_0)$. In addition, non-aligned scatterers were assumed which are described by $\mu_s' = 1\,\mathrm{mm}^{-1}$ and a Henyey-Greenstein scattering function with $g = 0.8$. The other optical coefficients were $\mu_a = 0.01\,\mathrm{mm}^{-1}$ and $n = 1.5$. The thickness of the slab was 10 mm. Further, the corresponding results from the anisotropic diffusion equations are shown ($\mu_{sz}' = 1.0\,\mathrm{mm}^{-1}$, $\mu_{sr}' = 1.0/1.75/2.5/4.0\,\mathrm{mm}^{-1}$). In addition, for a concentration of c_0 also the results obtained from the second Monte Carlo code (MC 2) are given.

Fitting the solutions of the isotropic diffusion equation to the results obtained by the Monte Carlo method does not deliver useful results for the reduced scattering coefficients [31, 32]. Similar results are obtained by applying the anisotropic diffusion equation if no additional information is known.

3.2. Time-state Domain

In this subsection we first present the results obtained for model 1 and then models 2 and 3 are considered. For all nonlinear regressions reported in this study the fitting range

was between the time of the maximum of the time-resolved reflectance or transmittance and the time where these quantities were decreased by a factor of 1000 compared to the maximum. Poisson noise was assumed to calculate the weights in the fitting routine. In an earlier study we showed that the absorption coefficient of a structural anisotropic semi-infinite medium can be obtained relatively precisely from time resolved reflectance measurement using solutions of the isotropic diffusion equation [31]. We repeated this approach for the time resolved reflectance from a semi-infinite medium of model 1 using a cylinder concentration of c_0 for different distances from the source (data not shown). The obtained absorption coefficient was within 5% of the real value of $\mu_a = 0.01\,\mathrm{mm}^{-1}$ for distances larger than 5 mm. For this distance range the reduced scattering coefficient was found to be between $\mu'_s = 2.55 - 2.7\,\mathrm{mm}^{-1}$. Thus, the values were within 8% of the value of the reduced scattering coefficient in lateral direction obtained in the last section ($\mu'_{sr} = 2.5\,\mathrm{mm}^{-1}$).

Fig. 5 presents the comparison of the time resolved transmittance from a slab with a thickness of 10 mm calculated with the Monte Carlo method (solid curves) and the anisotropic diffusion theory (dotted curves). Model 1 was applied with a concentration c_0 of the tubules using again $\mu'_{sx} = \mu'_{sy} = 1.5\,\mathrm{mm}^{-1}$ and $\mu'_{sz} = 0\,\mathrm{mm}^{-1}$ to describe the scattering by the tubules. Results for 5 different distances are shown, see legend. The figure confirms that diffusion theory is, in general, not a good approximation of the radiative transport theory for very early time values. Smaller systematic errors can also be seen for large time values.

We derived the optical properties fitting the solutions of the diffusion equation to the Monte Carlo simulations obtained from the turbid medium presented in Fig. 5 for different distances from the source. The obtained absorption coefficient and the derived reduced scattering coefficients are depicted in Fig. 6 and Fig. 7, respectively. First, the solution of the isotropic diffusion equation was fitted to the Monte Carlo data (black curves for transmittance and blue curves for reflectance data). In contrast to the semi-infinite case, the derived absorption coefficients have significant differences to the value used in the Monte Carlo method. However, for the time resolved transmittance determined at the opposite side of the incident source ($x = y = 0$mm) the absorption coefficient can be obtained with a relatively small error of about 15%. This error is mainly caused by the finite thickness of the slabs which causes a deterioration of the results obtained from diffusion theory. Interestingly, the reduced scattering coefficient derived at this location is within a few percent of the expected value ($\mu'_{sz} = 1.0\,\mathrm{mm}^{-1}$). According to the solution of the diffusion theory, see equation 1, this is anticipated because the shape of the time resolved transmittance depends only on μ'_{sz} and not on the other reduced scattering coefficients [14]. With increasing distances the derived reduced scattering coefficient (black curve in Fig. 7) increases up to a value close to $2.5\,\mathrm{mm}^{-1}$ which corresponds to the expected value of μ'_{sr}. Thus, performing measurement at zero distance and at a distance much larger than the thickness of the slab might allow to derive both involved reduced scattering coefficients. However, the absorption coefficient cannot be obtained precisely in this case. On the other hand, if μ'_{sz} has been correctly

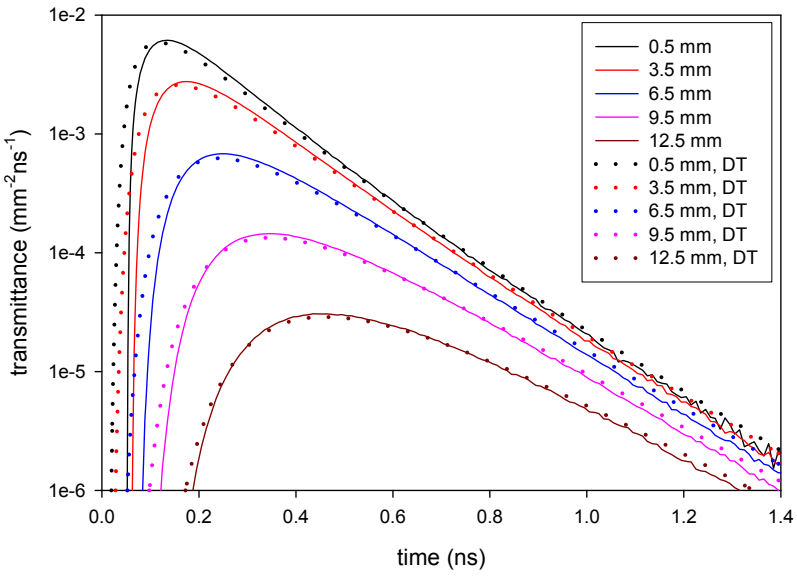

Figure 5. Time resolved transmittance from a turbid slab consisting of aligned tubules in z-direction at different distances from the incident $\delta(\rho, t)$-source. Calculations were performed with the Monte Carlo method for a cylinder concentration of c_0. In addition, non-aligned scatterers were assumed which were described by $\mu_s' = 1\,\mathrm{mm}^{-1}$ and a Henyey-Greenstein scattering function with $g = 0.8$. The other optical coefficients were $\mu_a = 0.01\,\mathrm{mm}^{-1}$ and $n = 1.5$. The thickness of the slab was 10 mm. For the calculations with the diffusion theory the following reduced scattering coefficients were used: $\mu_{sx}' = 2.5\,\mathrm{mm}^{-1}$, $\mu_{sy}' = 2.5\,\mathrm{mm}^{-1}$, $\mu_{sz}' = 1.0\,\mathrm{mm}^{-1}$.

derived from the measurement at zero distance, the solution of the anisotropic diffusion equation can be used to fit, besides the absorption coefficient, μ_{sr}'. The obtained results are also shown in Figs. 6 and 7, where it can be seen that μ_a and μ_{sr}' can be determined within an error of about $10-15\%$ for not too small distances. In addition, the retrieved values of the absorption coefficient are much more correct than those obtained by the isotropic diffusion equation. We remark that in these figures as well as in some of the following the derived optical properties are influenced by the noise of the Monte Carlo simulations especially at large distances (close to 20 mm).

The prediction of the anisotropic diffusion equation that the shape of the time resolved transmittance measured at the opposite side of the incident pencil beam does only depend on μ_{sz}' and on μ_a, but not on μ_{sx}' and μ_{sy}', was investigated with Monte Carlo simulations for model 1, see Fig. 8. The time resolved transmittance can be seen for two concentrations, c_0 and $c_0/2$, of the cylinders. In order to be able to compare precisely the shape of both curves the curve for $c_0/2$ was multiplied by 1.4. The figure shows that the two curves match very well indicating that also within transport theory the shape of the curves are the same. We note that a multiplicative constant of 1.4 corresponds to reduced scattering coefficients describing the cylindrical tubules with $\mu_{sx}' = \mu_{sy}' = 1.33\,\mathrm{mm}^{-1}$ and $\mu_{sz}' = 0\,\mathrm{mm}^{-1}$, compare Eq. 3. Thus, the value for μ_{sr}' is more than 10% lower than the optimal μ_{sr}' found for Figs. 3 and 4.

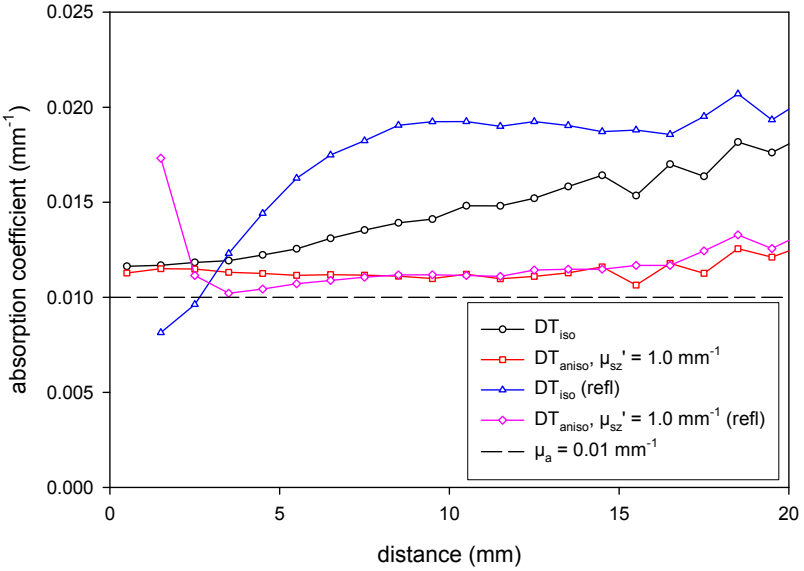

Figure 6. Absorption coefficients obtained by fitting time resolved transmittance and reflectance from turbid slabs consisting of aligned tubules directed in z-direction at different distances from the incident $\delta(\rho, t)$-source. In the fitting routine the isotropic diffusion equation and the anisotropic diffusion equation with $\mu'_{sz} = 1.0\,\mathrm{mm}^{-1}$ were used as forward solutions, see legend. In addition, the absorption coefficient used in the Monte Carlo simulations is depicted ($\mu_a = 0.01\,\mathrm{mm}^{-1}$). The thickness of the turbid media was $d = 10\,\mathrm{mm}$.

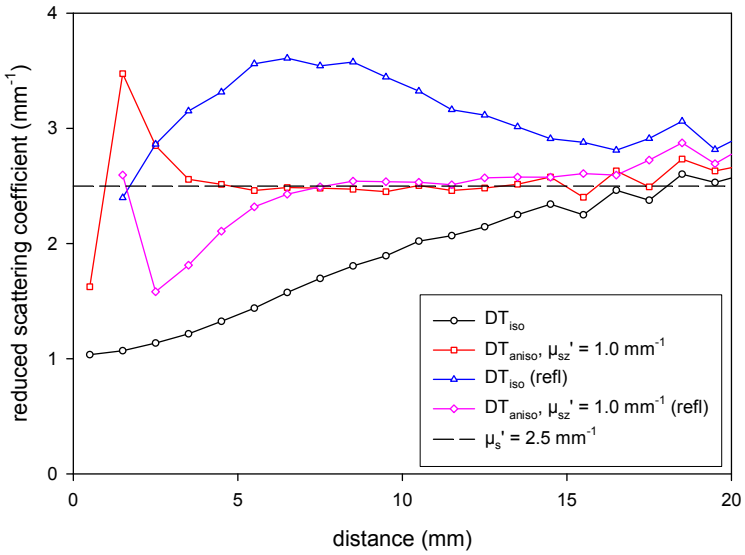

Figure 7. Reduced scattering coefficients obtained by fitting time resolved transmittance and reflectance from turbid slabs consisting of aligned tubules directed in z-direction at different distances from the incident $\delta(\rho, t)$-source. In the fitting routine the isotropic diffusion equation and the anisotropic diffusion equation with $\mu'_{sz} = 1.0\,\mathrm{mm}^{-1}$ were used as forward solutions, see legend. In addition, the reduced scattering coefficient of $\mu'_s = 2.5\,\mathrm{mm}^{-1}$ is depicted. The thickness of the turbid media was $d = 10\,\mathrm{mm}$.

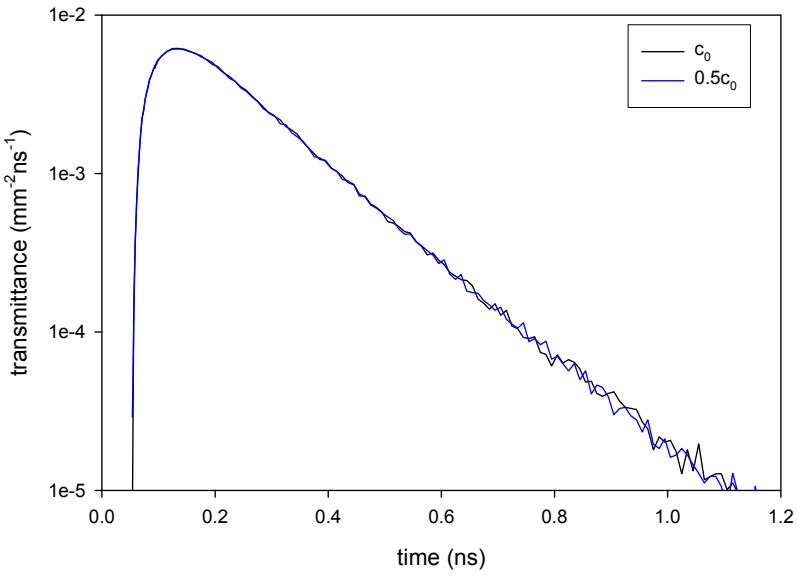

Figure 8. Time resolved transmittance from a turbid slab consisting of aligned tubules in z-direction opposite to the incident $\delta(\rho, t)$-source. Calculations were performed with the Monte Carlo method for two different cylinder concentrations $(c_0, c_0/2)$. In addition, non-aligned scatterers were assumed which are described by $\mu_s' = 1\,\mathrm{mm}^{-1}$ and a Henyey-Greenstein scattering function with $g = 0.8$. The other optical coefficients were $\mu_a = 0.01\,\mathrm{mm}^{-1}$ and $n = 1.5$. The thickness of the slab was 10 mm. The curve with the smaller concentration $(c_0/2)$ was multiplied by 1.4.

In the second part of this section we consider the light propagation in structurally anisotropic scattering media described by models 2 and 3. Fig. 9 and Fig. 10 show a comparison of the time resolved reflectance from a semi-infinite medium of model 3 at a distance of 4.5 mm and 14.5 mm from the source, respectively. The reflectance was calculated in different directions, ϕ, relative to the x-axis using the Monte Carlo method (solid curves) and the solution of anisotropic diffusion equation (dotted curves). For the diffusion theory based data the known absorption coefficient and the reduced scattering coefficients assuming $\mu_{sz}' = 1.5\,\mathrm{mm}^{-1}$ were used. Due to the fact that 75% of the cylinders are aligned in x- and 25% in y-direction it follows that $\mu_{sx}' = 0.375\,\mathrm{mm}^{-1}$, $\mu_{sy}' = 1.125\,\mathrm{mm}^{-1}$. At a distance of 4.5 mm the maximum of the time resolved reflectance is, at first, decreasing and then increasing when the reflectance is determined at increasing ϕ-values $(\phi = 10, 30, 50, 70, 90°)$. This is consistent with the steady-state iso-intensity contour lines (data not shown) which show qualitatively similar reflectance patterns as those for the corresponding slab medium, compare Fig. 2. In contrast, diffusion theory shows just a decreasing maximum with increasing ϕ-values. Contrarily, at a distance of 14.5 mm the results obtained from the Monte Carlo method show a decrease of the reflectance maximum as is predicted by diffusion theory. We note, however, that, quantitatively, there are differences especially for large ϕ-values. Especially, at these ϕ-values a better agreement was achieved for smaller reduced scattering coefficients e.g. $\mu_{sx}' = 0.35\,\mathrm{mm}^{-1}$, $\mu_{sy}' = 1.15\,\mathrm{mm}^{-1}$, $\mu_{sz}' = 1.4\,\mathrm{mm}^{-1}$ (data

not shown).

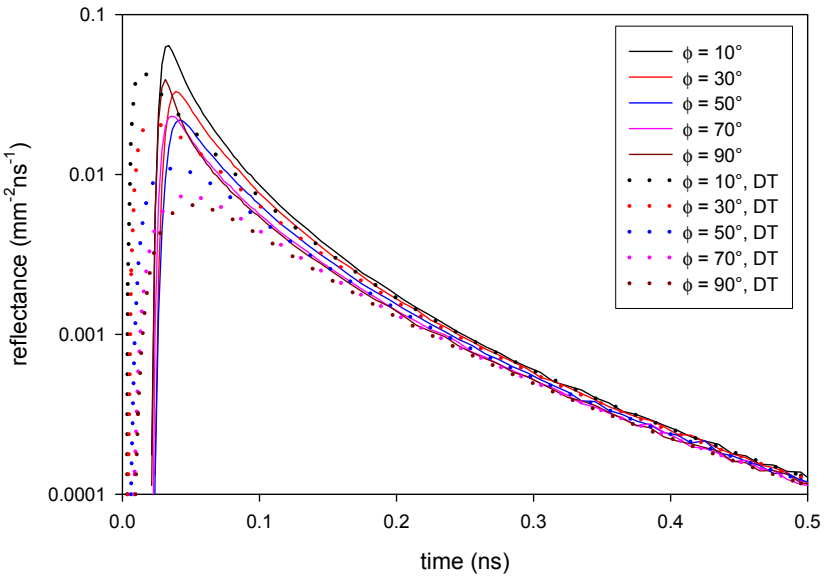

Figure 9. Time resolved reflectance from semi-infinite turbid media consisting of aligned tubules (75% in x- and 25% in y-direction) at a distance of 4.5 mm from the incident $\delta(\rho, t)$-source. Calculations were performed with the Monte Carlo method and the diffusion theory for different directions ϕ. The optical coefficients used for the diffusion theory were $\mu'_{sx} = 0.375\,\mathrm{mm}^{-1}$, $\mu'_{sy} = 1.125\,\mathrm{mm}^{-1}$, $\mu'_{sz} = 1.5\,\mathrm{mm}^{-1}$, $\mu_a = 0.01\,\mathrm{mm}^{-1}$, and $n = 1.5$.

The time resolved transmittance from slabs of model 3 show for small and large distances, qualitatively, an agreement of the results obtained by diffusion theory and Monte Carlo simulations, however, quantitatively the disagreement is similar as in Fig. 10 (data not shown).

In the following the absorption and reduced scattering coefficients obtained by fitting the isotropic and anisotropic diffusion equations to Monte Carlo simulations at different distances between the incident source and the detection location are shown. Fig. 11 and Fig. 12 present the absorption and reduced scattering coefficients, respectively, for model 2 using a semi-infinite geometry. A concentration of $c_0/2$ is used for the cylinders aligned both in the x- and the y-directions. In the Monte Carlo simulation no discrimination in the ϕ-angle was considered in order to improve the statistics. This is not possible anymore for model 3 because of the pronounced anisotropic reflectance pattern. The nonlinear regressions applying the solution of the isotropic diffusion equation deliver an absorption coefficient within 5% compared to the true value of $\mu_a = 0.01\,\mathrm{mm}^{-1}$ for distances larger than 10 mm, whereas the reduced scattering coefficient is relatively low at about $\mu'_s = 0.4\,\mathrm{mm}^{-1}$ at small distances increasing towards $\mu'_s = 0.8\,\mathrm{mm}^{-1}$ for large distances. Next the anisotropic diffusion theory was fitted to the Monte Carlo data using the knowledge that the same number of cylinders are aligned in x- and y-directions, which results in $\mu'_{sz} = 2\mu'_{sx} = 2\mu'_{sy}$. The obtained absorption coefficients are within 5% of the true absorption coefficient

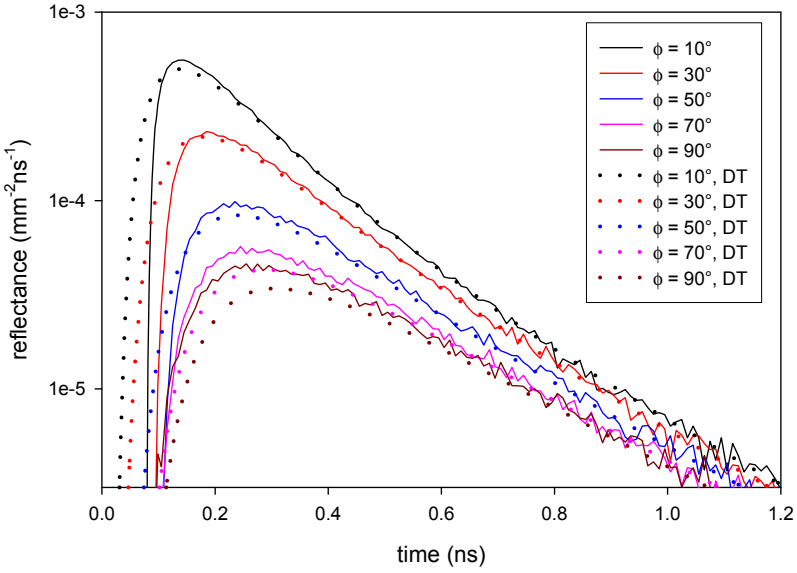

Figure 10. Time resolved reflectance from semi-infinite turbid media consisting of aligned tubules (75% in x- and 25% in y-direction) at a distance of 14.5 mm from the incident $\delta(\rho, t)$-source. Calculations were performed with the Monte Carlo method and the diffusion theory for different directions ϕ. The optical coefficients used for the diffusion theory were $\mu'_{sx} = 0.375\,\mathrm{mm}^{-1}$, $\mu'_{sy} = 1.125\,\mathrm{mm}^{-1}$, $\mu'_{sz} = 1.5\,\mathrm{mm}^{-1}$, and $n = 1.5$.

already at distances larger than 7 mm. Similar, the reduced scattering coefficients μ'_{sr} are increasing already at smaller distances to a value close to $\mu'_{sr} = 0.8\,\mathrm{mm}^{-1}$. For the case that a previous knowledge of the geometrical alignment of the cylindrical microstructure is not known we investigated a third approach. We assumed that μ'_{sz} can be determined successfully with time resolved transmission measurements. Accordingly, we fixed μ'_{sz} to the value obtained below ($\mu'_{sz} = 1.7\,\mathrm{mm}^{-1}$, see Fig. 14). The fitted μ'_{sr} and μ_a are given in the figures showing that the values at larger distances are again approximated already at smaller distances compared to the results obtained with the isotropic diffusion theory.

Fig. 11 and Fig. 12 show the retrieved absorption and reduced scattering coefficients not only for cylinders representing the tubules in dentin but also for those representing the collagen fibers in tendon. The concentration of the collagen cylinders was chosen so that the same reduced scattering coefficients were obtained as for the tubule cylinders using the c_0-concentration according to [36]. In principle, the fitted optical properties show the same behavior versus distance from the source, but the expected values were obtained even at smaller distances.

Next, we present the absorption and reduced scattering coefficients retrieved by fitting diffusion theory to time resolved reflectance from a semi-infinite medium obtained from Monte Carlo simulations of model 3, see Figs. 13 and 14. Due to the anisotropic light propagation caused by the microstructure of model 3, compare Fig. 2, the reflectance data have to be considered for different angles ϕ separately. The figures

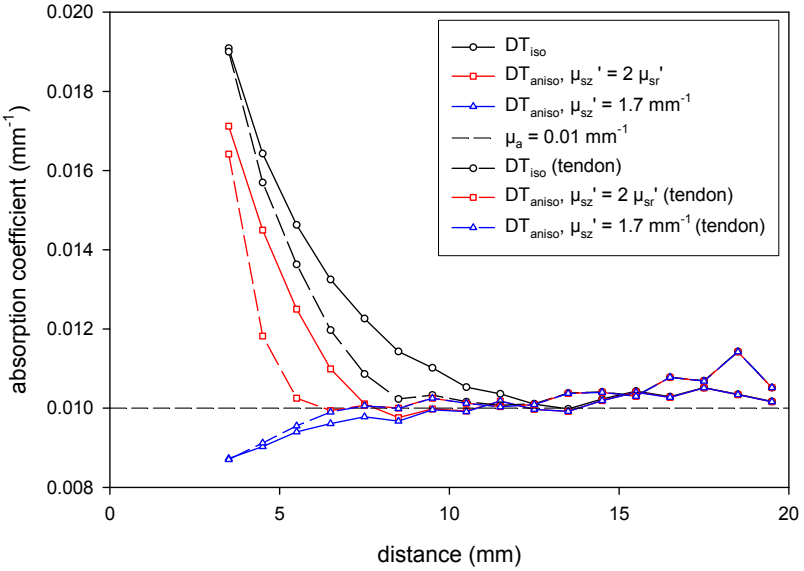

Figure 11. Absorption coefficients obtained by fitting time resolved reflectance from semi-infinite turbid media consisting of aligned tubules (50% in x- and 50% in y-direction) at different distances from the incident $\delta(\rho, t)$-source. In the fitting routine the isotropic diffusion equation and the anisotropic diffusion equation with $\mu'_{sz} = 2\mu'_{sr}$ and $\mu'_{sz} = 1.7\,\mathrm{mm}^{-1}$ were used as forward solutions, see legend. In addition, the absorption coefficient used in the Monte Carlo simulations is depicted ($\mu_a = 0.01\,\mathrm{mm}^{-1}$). Besides fitting results for the tubules also those for collagen cylinders in tendon are given.

show data in y-direction ($\phi = 90°$; in the Monte Carlo simulations: $\phi = 80° - 100°$) and approximately in x-direction ($\phi = 10°$; in the Monte Carlo simulations: $\phi = 0° - 20°$). Fitting the isotropic diffusion equation the true value of the absorption coefficient is approximately obtained already for relatively small distances for $\phi = 90°$, whereas for $\phi = 10°$ $\mu_a = 0.01\,\mathrm{mm}^{-1}$ is slowly approached at large distances. We emphasize that the statistics of the Monte Carlo simulations are worse for model 3 because the data cannot be averaged over the different ϕ-angles. This can be seen by the noise of the fitted optical properties especially at $\phi = 90°$ and at large distances, because in this direction the decrease of the reflectance is much larger relative to the reflectance at $\phi = 10°$, compare Fig. 2. This larger decrease is caused by the larger reduced scattering coefficient in this direction, which is also the reason why the isotropic diffusion equation is able to approach the real values at shorter distances compared to the calculation at $\phi = 10°$. A similar behavior can be observed for the obtained reduced scattering coefficients. At $\phi = 90°$ the fitted reduced scattering coefficient approaches the expected value of $0.75 \cdot 1.70\,\mathrm{mm}^{-1} = 1.275\,\mathrm{mm}^{-1}$ already at about 15 mm, whereas at $\phi = 10°$ the expected value of $0.25 \cdot 1.70\,\mathrm{mm}^{-1} = 0.425\,\mathrm{mm}^{-1}$ is not reached within distances of 20 mm.

The figures show also the fitted optical properties obtained by the anisotropic diffusion theory. Again, we assumed that the reduced scattering coefficient μ'_{sz} is known ($\mu'_{sz} = 1.7\,\mathrm{mm}^{-1}$). Thus, besides the absorption coefficient μ'_{sr} was fitted at $\phi = 10°$

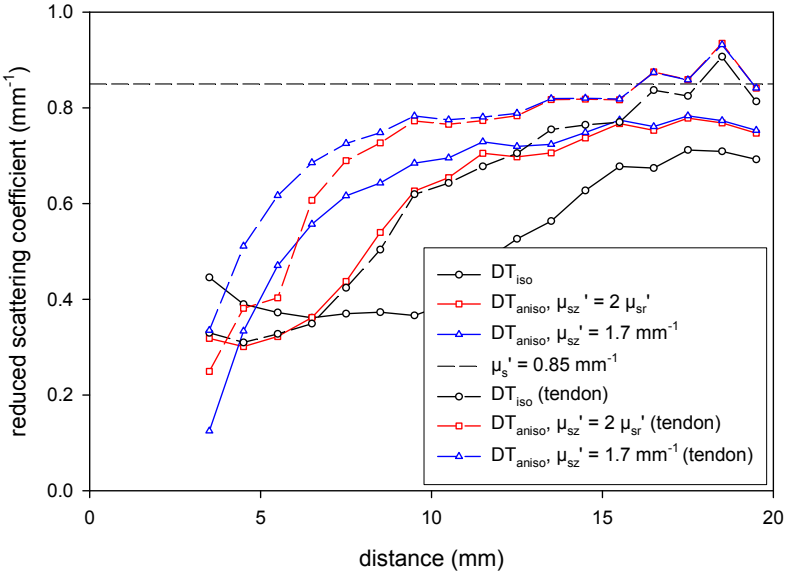

Figure 12. Reduced scattering coefficients obtained by fitting time resolved reflectance from semi-infinite turbid media consisting of aligned tubules (50% in x- and 50% in y-direction) at different distances from the incident $\delta(\rho, t)$-source. In the fitting routine the isotropic diffusion equation and the anisotropic diffusion equation with $\mu'_{sz} = 2\mu'_{sr}$ and $\mu'_{sz} = 1.7\,\mathrm{mm}^{-1}$ were used as forward solutions, see legend. In addition, the reduced scattering coefficient of $\mu'_s = 0.85\,\mathrm{mm}^{-1}$ is depicted. Besides fitting results for the tubules also those for collagen cylinders in tendon are given.

and $\phi = 90°$. It can be seen that, similar as for model 2, the expected optical properties are now approached already at relatively small distances to the source.

Finally, the derived optical properties retrieved by fitting Monte Carlo simulations for the time-resolved transmittance from a slab with a thickness of 10 mm are presented. Figs. 15 and 16 show the absorption and reduced scattering coefficients obtained for model 2. As discussed above, at least in the diffusion approximation the transmittance obtained at the opposite location of the incident beam does only depend on μ'_{sz} and μ_a. The figures show that using the isotropic diffusion equation a reduced scattering coefficient of $\mu'_{sz} = 1.7\,\mathrm{mm}^{-1}$ is obtained. Thus, this value is applied for some of the fitting results presented in this section. The obtained absorption coefficient has a difference of about 12% compared to the exact value of $\mu_a = 0.01\,\mathrm{mm}^{-1}$. Besides statistical noise this is most probably caused by the finite thickness of the slab which deteriorates the diffusion approximation. Consequently, also the value of $\mu'_{sz} = 1.7\,\mathrm{mm}^{-1}$ obtained above by using the diffusion theory has some uncertainty. We note, however, that we recently derived an exact analytical solution of the radiative transport equation which can be applied to get, in principle, exact values [39].

For larger distances the reduced scattering coefficient obtained from the isotropic diffusion equation is approaching the expected value of $\mu'_{sr} = 0.5 \cdot 1.7\,\mathrm{mm}^{-1} = 0.85\,\mathrm{mm}^{-1}$, because, obviously, the influence of μ'_{sr} compared to μ'_{sz} on the time resolved transmittance curve is increased. However, the absorption coefficient shows significant

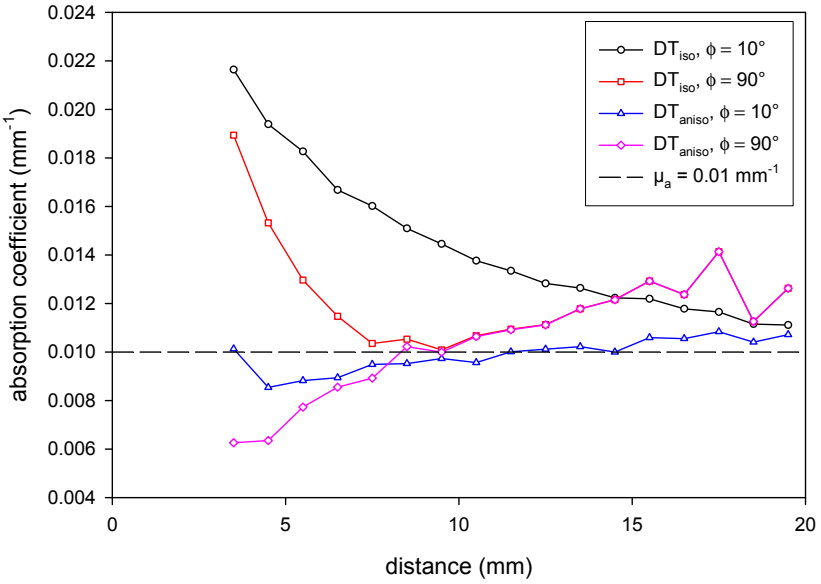

Figure 13. Absorption coefficients obtained by fitting time resolved reflectance from semi-infinite turbid media consisting of aligned tubules (75% in x- and 25% in y-direction) at different distances from the incident $\delta(\rho, t)$-source and for different ϕ-directions. In the fitting routine the isotropic diffusion equation and the anisotropic diffusion equation with $\mu'_{sz} = 1.7\,\mathrm{mm}^{-1}$ were used, see legend. In addition, the absorption coefficient applied in the Monte Carlo simulations is depicted ($\mu_a = 0.01\,\mathrm{mm}^{-1}$).

differences to the true value. This feature that, in contrast to semi-infinite media, the absorption coefficient of slabs (both for time resolved reflectance and transmittance measurements) cannot be determined precisely with the isotropic diffusion equation was observed generally.

Again, the optical properties were fitted with the anisotropic diffusion theory applying two kinds of previous knowledge. In the first the previous knowledge is used that $\mu'_{sz} = 2\mu'_{sx} = 2\mu'_{sy}$ and for the second it was assumed that μ'_{sz} is known ($\mu'_{sz} = 1.7\,\mathrm{mm}^{-1}$). As above the additional knowledge improves the results of the nonlinear regression. The absorption coefficient has an average error of less than 10% for all distances and both kinds of previous knowledge, whereas the expected value for the reduced scattering coefficient is now approached already at smaller distances.

Figs. 17 and 18 give the retrieved absorption and reduced scattering coefficients for the corresponding time resolved transmittance measurements from a slab of a thickness of 10 mm for model 3 and for $\phi = 10°$ and $\phi = 90°$. The derived absorption coefficient shows, in general, a bit larger differences compared to model 2, which is mainly caused by the worse statistics as discussed above. The reduced scattering coefficients obtained by the isotropic diffusion equation approach the expected values at large distances for both values of ϕ. Using the solution of the anisotropic diffusion equation and applying the assumption that $\mu'_{sz} = 1.7\,\mathrm{mm}^{-1}$ the figure shows that, especially for $\phi = 10°$, the expected reduced scattering coefficient can be obtained already at much shorter

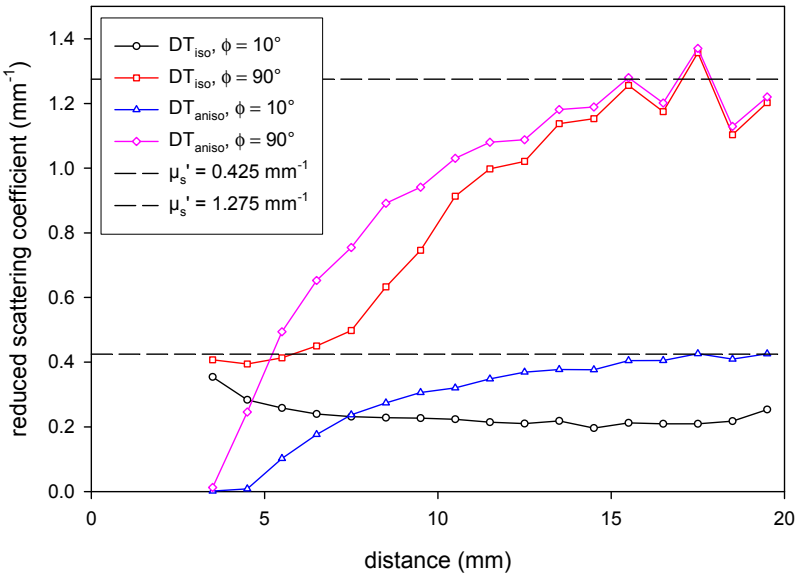

Figure 14. Reduced scattering coefficients obtained by fitting time resolved reflectance from semi-infinite turbid media consisting of aligned tubules (75% in x- and 25% in y-direction) at different distances from the incident $\delta(\rho, t)$-source and for different ϕ-directions. In the fitting routine the isotropic diffusion equation and the anisotropic diffusion equation with $\mu'_{sz} = 1.7\,\mathrm{mm}^{-1}$ were used, see legend. In addition, the reduced scattering coefficients of $\mu'_s = 0.425\,\mathrm{mm}^{-1}$ and $\mu'_s = 1.275\,\mathrm{mm}^{-1}$ are depicted.

distances.

4. Summary and Conclusions

In this study the light propagation in structural anisotropic media was described using the Monte Carlo method and solutions of the isotropic and anisotropic diffusion equations. The applied Monte Carlo code was successfully validated in the time domain (not shown) and in the steady-state domain (Fig. 4) against a second Monte Carlo code which was completely independently written by the authors. Three different arrangements of the aligned microstructure were considered for two different cylindric fibers. The results were mainly shown for the dentinal tubules, however, those for the collagen fibers delivered, in principle, the same results.

By comparing the forward calculations of the Monte Carlo method and the solutions of the anisotropic diffusion theory in the steady-state and time domains using the same absorption coefficient a good agreement could be achieved at large distances from the source by varying the reduced scattering coefficients in the solution of the anisotropic diffusion equation. However, different quantitative values for the reduced scattering coefficients were obtained for the investigated models and measurement domains. Namely, the derived reduced scattering coefficient in direction perpendicular to the cylindric tubules varied between $1.33 - 1.7\,\mathrm{mm}^{-1}$. Thus, the anisotropic diffusion

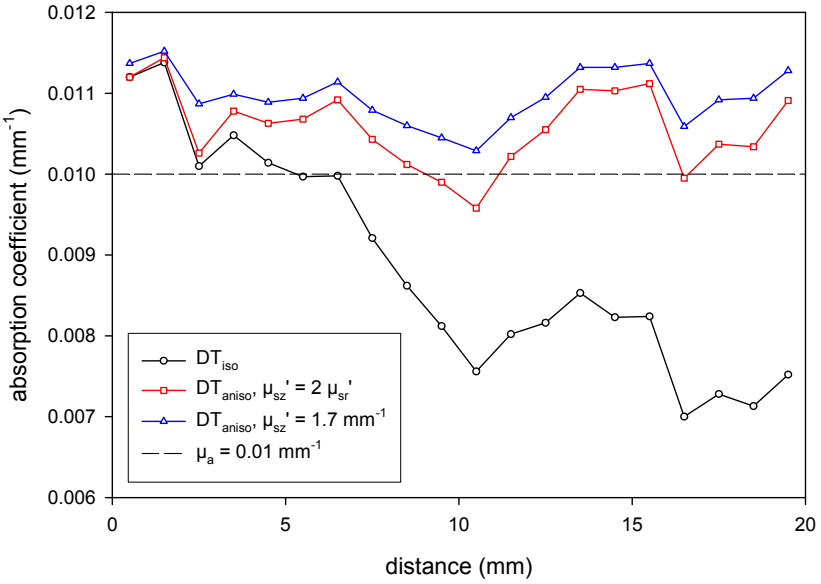

Figure 15. Absorption coefficients obtained by fitting time resolved transmittance from turbid media consisting of aligned tubules (50% in x- and 50% in y-direction) at different distances from the incident $\delta(\rho, t)$-source. In the fitting routine the isotropic diffusion equation and the anisotropic diffusion equation with $\mu'_{sz} = 2\mu'_{sr}$ and $\mu'_{sz} = 1.7\,\mathrm{mm}^{-1}$ were used, see legend. In addition, the absorption coefficient applied in the Monte Carlo simulations is depicted ($\mu_a = 0.01\,\mathrm{mm}^{-1}$). The thickness of the turbid media was $d = 10\,\mathrm{mm}$.

theory shows systematic errors not only at small distances where it is expected but also at larger distances or longer time values.

For small distances from the source the anisotropic diffusion theory delivers wrong results not only quantitatively but also qualitatively. Whereas in the steady-state domain this was already shown before [31], in the time domain it was described in this study, compare Fig. 9. Nevertheless, we also found that nonlinear regressions using the solutions of both the isotropic and the anisotropic diffusion equations deliver useful results for the retrieved optical properties.

Using the isotropic diffusion theory we could confirm our earlier result that the absorption coefficient can be successfully obtained by time resolved reflectance measurements from semi-infinite media [31]. Additionally, in the present study we found that at large distances ($\gg 1/\mu'_s$) from the source the fitted reduced scattering coefficients approach the expected value for the considered ϕ-angle enabling, in principle, the derivation of μ'_{sx} and μ'_{sy}. Based on previous knowledge of the microstructure of the investigated scattering media, which is available in many cases, this allows to derive also μ'_{sz}. Contrarily, for slabs we found that the optical properties derived with the isotropic diffusion equation have relatively large errors compared to the actual values.

The investigations using the anisotropic diffusion equation in the time domain showed that, in general, better results can be obtained compared to the isotropic diffusion equation provided that some previous knowledge is available. We showed

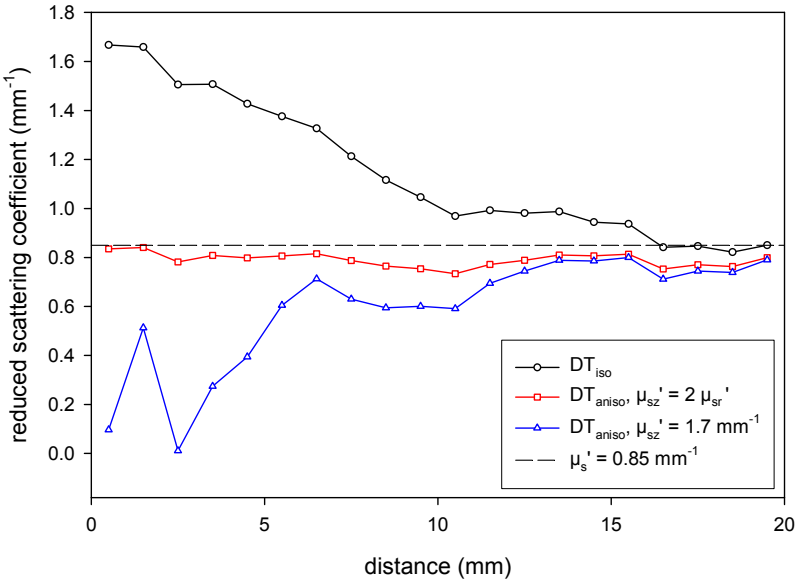

Figure 16. Reduced scattering coefficients obtained by fitting time resolved transmittance from turbid media consisting of aligned tubules (50% in x- and 50% in y-direction) at different distances from the incident $\delta(\rho, t)$-source. In the fitting routine the isotropic diffusion equation and the anisotropic diffusion equation with $\mu'_{sz} = 2\mu'_{sr}$ and $\mu'_{sz} = 1.7\,\mathrm{mm}^{-1}$ were used, see legend. In addition, the reduced scattering coefficient of $\mu'_s = 0.85\,\mathrm{mm}^{-1}$ is depicted. The thickness of the turbid media was $d = 10\,\mathrm{mm}$.

that, normally, the expected optical properties could be retrieved already at smaller distances compared to the case when the isotropic diffusion equation is used. We also found that μ'_{sz} can be obtained with relatively small errors by measuring the time resolved transmittance at the position opposite to the incident beam and using the isotropic diffusion theory. We found, further, using Monte Carlo simulations that this feature seems to be also valid in the framework of radiative transport theory. Thus, the results from this measurement can be improved by applying an analytical solution of the radiative transport equation for arbitrarily rotationally symmetric scattering functions, which we derived recently [39]. The application of the transport theory solution is even more important for slabs having a thickness which is not much larger than μ'_{sz}, because, in general, the diffusion approximation is worse for those cases.

In summary, we could show that although the isotropic and anisotropic diffusion theory have several qualitative and quantitative shortcomings compared to solutions of the radiative transfer theory, it can be successfully employed to obtain useful results for the determination of the optical properties of structurally anisotropic scattering media for several applications.

References

[1] A. Ishimaru: Wave Propagation and Scattering in Random Media (Academic Press, 1978).

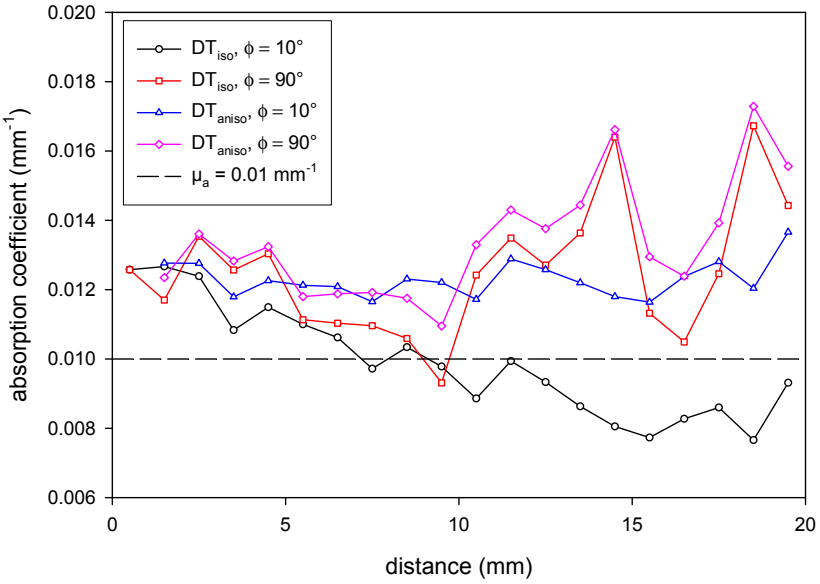

Figure 17. Absorption coefficients obtained by fitting time resolved transmittance from turbid media consisting of aligned tubules (75% in x- and 25% in y-direction) at different distances from the incident $\delta(\rho, t)$-source and for different ϕ-directions. In the fitting routine the isotropic diffusion equation and the anisotropic diffusion equation with $\mu'_{sz} = 1.7\,\mathrm{mm}^{-1}$ were used, see legend. In addition, the absorption coefficient applied in the Monte Carlo simulations is depicted ($\mu_a = 0.01\,\mathrm{mm}^{-1}$). The thickness of the turbid media was $d = 10\,\mathrm{mm}$.

[2] M.I Mishchenko, L.D. Travis, A.A. Lacis: Multiple Scattering of Light by Particles: Radiative Transfer and Coherent Backscattering (Cambridge U. Press, 2006).

[3] F. Martelli, S. Del Bianco, A. Ismaelli, G. Zaccanti: Light Propagation through Biological Tissue and Other Diffusive Media: Theory, Solutions, and Software (SPIE Press Book, 2009).

[4] M.H. Kao, K.A. Jester, A.G. Yodh, P.J. Collings: Observation of Light Diffusion and Correlation Tranport in Nematic Liquid Crystals, Phys. Rev. Lett. 77, 2233–2236 (1996).

[5] B.A. van Tiggelen, R. Maynard, A. Heiderich: Anisotropic Light Diffusion in Oriented Nematic Liquid Crystals, Phys. Rev. Lett. 77, 639–642 (1996).

[6] D.S. Wiersma, A. Muzzi, M. Colocci, R. Righini: Time-Resolved Aniostropic Multiple Scattering in Nematic Liquid Crystals, Phys. Rev. Lett. 83, 4321–4324 (1999).

[7] D.S. Wiersma, A. Muzzi, M. Colocci, R. Righini: Time-Resolved Experiments on Light Diffusion in Anisotropic Random Media, Phys. Rev. E 62, 6681–6687 (2000).

[8] B. Peng, T. Ding, P. Wang: Propagation of Polarized Light through Textile Material, Appl. Opt. 51, 6325–6334 (2012).

[9] S. Nickell, M. Hermann, M. Essenpreis, T.J. Farrell, U. Krämer, M.S. Patterson: Anisotropy of Light Propagation in Human Skin, Phys. Med. Biol. 45, 2873–2886 (2000).

[10] A. Sviridov, V. Chernomordik, M. Hassan, A. Russo, A. Eidsath, P. Smith, A. H. Gandjbakhche: Intensity Profiles of Linearly Polarized Light Backscattered from Skin and Tissue-like Phantoms, J. Biomed. Opt. 10, 014012 (2005).

[11] A. Kienle, F.K. Forster, R. Diebolder, R. Hibst: Light Propagation in Dentin: Influence of Microstructure on Anisotropy, Phys. Med. Biol. 48, N7–N14 (2003).

[12] T. Binzoni, C. Courvoisier, R. Giust, G. Tribillon, T. Gharbi, J.C. Hebden, T.S. Leung, J. Roux, D.T. Delpy: Anisotropic Photon Migration in Human Skeletal Muscle, Phys. Med. Biol. 51, N79–N90 (2006).

[13] A. Kienle, C. D'Andrea, F. Foschum, P. Taroni, A. Pifferi: Light Propagation in Dry and Wet

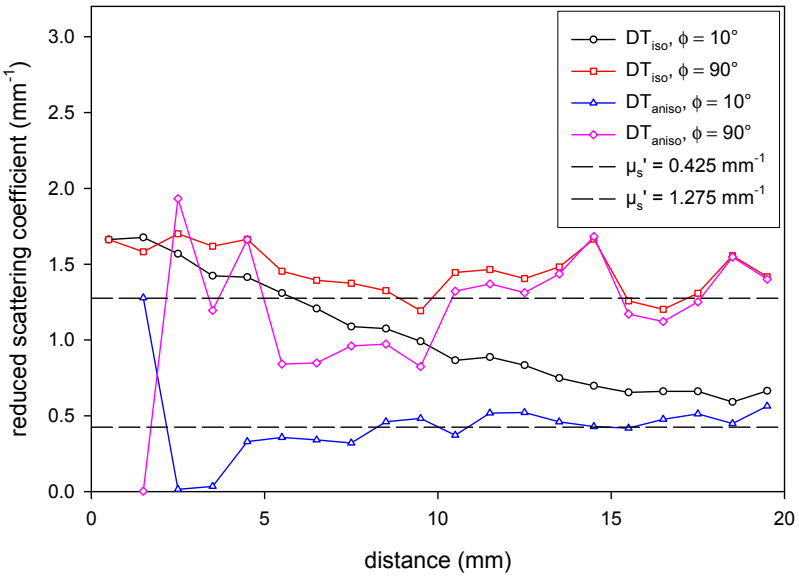

Figure 18. Reduced scattering coefficients obtained by fitting time resolved transmittance from turbid media consisting of aligned tubules (75% in x- and 25% in y-direction) at different distances from the incident $\delta(\rho, t)$-source and for different ϕ-directions. In the fitting routine the isotropic diffusion equation and the anisotropic diffusion equation with $\mu'_{sz} = 1.7\,\mathrm{mm}^{-1}$ were used, see legend. In addition, the reduced scattering coefficient of $\mu'_s = 0.425\,\mathrm{mm}^{-1}$ and $\mu'_s = 1.275\,\mathrm{mm}^{-1}$ are depicted. The thickness of the turbid media was $d = 10\,\mathrm{mm}$.

Soft Wood, Opt. Express 16, 9895–9906 (2008).

[14] P.M. Johnson, B.P.J. Bret, J.G. Rivas, J.J. Kelly, Ad Lagendijk: Anisotropic Diffusion of Light in a Strongly Scattering Material, Phys. Rev. Lett. 89, 243901 (2002).

[15] H. Stark, T.C. Lubensky: Multiple Light Scattering in Nematic Liquid Crystals, Phys. Rev. Lett. 77, 2229–2232 (1996).

[16] H. Stark, T.C. Lubensky: Multiple Light Scattering in Anisotropic Random Media, Phys. Rev. E 55, 514–533 (1996).

[17] J. Heino, S. Arridge, J. Sikora, E. Somersalo: Anisotropic Effects in Highly Scattering Media, Phys. Rev. E 68, 031908 (2003).

[18] O.K. Dudko, G.H. Weiss: Estimation of Anisotropical Optical Parameters of Tissue in a Slab Geometry, Biophys. J. 88, 3205–3211 (2005).

[19] O.K. Dudko, G.H. Weiss, V. Chernomordik, A.H. Gandjbakhche: Estimation of Anisotropic Optical Parameters of Tissue in a Slab Geometry, Phys. Med. Biol. 49, 3979-3989 (2004).

[20] A. Kienle, F.K. Forster, R. Hibst: Anisotropy of Light Propagation in Biological Tissue, Opt. Lett. 29, 2617–2619 (2004).

[21] T. Yun, N. Zeng, W. Li, D. Li, X. Jiang, H. Ma: Monte Carlo Simulation of Polarized Photon Scattering in Anisotropic Media, Opt. Exp. 17, 16590–16602 (2009).

[22] C. Fan, A. Shuaib, G. Yao: Path-length Resolved Reflectance in Tendon and Muscle, Opt. Exp. 19, 8879–8887 (2011).

[23] T. Linder, T. Loefqvist: Monte Carlo Simulation of Photon Transport in a Randomly Oriented Sphere-Cylinder Scattering Medium, Appl. Physics. B 105, 659-664 (2011).

[24] N. Moumini, C. Baravian: Incoherent Light Transport in Anisotropic Media: Form Factor Influence for Oriented Prolate Ellipsoids, J. Quant. Spectrosc. Radiat. Transfer 110, 1545-1565 (2009).

[25] L. Dagdug, G.H. Weiss, A.H. Gandjbakhche: Effects of Anisotropic Optical Properties on Photon

Migration in Structured Tissue, Phys. Med. Biol. 48, 1361–1370 (2003).

[26] W. Jakob, A. Arbree, J.T. Moon, K. Bala, S. Marschner: A Radiative Transfer Framework for Rendering Materials with Anisotropic Structure, ACM Transactions on Graphics 29, 53 (2010).

[27] L. Margerin: Attenuation, Transport and Diffusion of Scalar Waves in Textured Random Media, Tectonophysics 416, 229-244 (2006).

[28] P.M. Johnson, S. Faez, A. Lagendijk: Full Characterization of Anisotropic Diffuse Light, Opt. Express 16, 7436–7446 (2008).

[29] E. Alerstam, T. Svensson: Observation of Anisotropic Diffusion of Light in Compacted Granular Porous Materials, Phys. Rev. E 85, 040301(R) (2012).

[30] E. Alerstam: Optical Spectroscopy of Turbid Media: Time-Domain Measurements and Accelerated Monte Carlo modelling, Doctoral thesis, Lund University, Sweden (2011).

[31] A. Kienle, C. Wetzel, A. Bassi, D. Comelli, P. Taroni, A. Pifferi: Determination of the Optical Properties of Anisotropic Biological Media using an Isotropic Model, J. Biomed. Opt. 12, 014026 (2007).

[32] A. Kienle: Anisotropic Light Diffusion: An Oxymoron?, Phys. Rev. Lett. 98, 218104 (2007).

[33] F. Voit, A. Hohmann, J. Schäfer, A. Kienle: Multiple Scattering of Polarized Light: Comparison of Maxwell Theory and Radiative Transfer Theory, J. Biomed.Opt. 17, 045003 (2012).

[34] H.A. Yousif, E. Boutros:, "A FORTRAN Code for the Scattering of EM Plane Waves by an Infinitely Long Cylinder at Oblique Incidence," Comput. Phys. Commun. **69**, 406–414 (1992).

[35] R.C. Haskell, L.O. Svaasand, T.T. Tsay, T.C. Feng, M. McAdams, B.J. Tromberg: Boundary Conditions for the Diffusion Equation in Radiative Transfer, J. Opt. Soc. Am. A 11, 2727–2741 (1994).

[36] P.M. Johnson, A. Lagendijk: Optical Anisotropic Diffusion: New Model Systems and Theoretical Modeling, J. Biomed. Opt. 14, 054036 (2009).

[37] A. Kienle, M.S. Patterson: Improved Solutions of the Steady-State and the Time-Resolved Diffusion Equations for Reflectance from a Semi-Infinite Turbid Medium, J. Opt. Soc. Am. A 14, 246–254 (1997).

[38] A. Kienle, R. Hibst: Light Guiding in Biological Tissue due to Scattering, Phys. Rev. Lett. 97, 018104 (2006).

[39] A. Liemert, A. Kienle: Exact and Efficient Solution of the Radiative Transport Equation for the Semi-Infinite Medium, Scientific Reports, accepted (2013).